

EXPERIMENTAL INVESTIGATION OF TURBULENT HEAT TRANSFER AND FLUID FLOW IN INTERNALLY FINNED TUBES WITH SURFACE ROUGHNESS

Je H. Kim and Michael K. Jensen

Department of Mechanical Engineering, Aeronautical Engineering and Mechanics
Rensselaer Polytechnic Institute
Troy, NY 12180
U. S. A.

ABSTRACT

An experimental investigation of simultaneously developing, steady, turbulent flow under heating conditions in both straight and helically finned tubes with surface roughness (sand grain type) has been performed. Length-averaged heat transfer and pressure drop were obtained using air as the test fluid in twelve rough fin tubes and one rough tube without fins. Adiabatic friction factors and Nusselt numbers were measured for fin geometries of $18 \leq N \leq 60$, $0.056 \leq H \leq 0.269$, $7.562 \mu\text{m} \leq Ra_{11} \leq 14.941 \mu\text{m}$ and $0^\circ \leq \gamma \leq 26^\circ$. Turbulent flow operating conditions ranged from $7,500 < Re < 43,000$ and $Pr \approx 0.7$. In addition, adiabatic friction factors were obtained for the range $9,100 < Re < 54,000$ using ambient air at the test fluid. The results are compared to existing smooth fin tube correlations. The rough fin tube results exhibited substantial increases in friction factors while corresponding increases in Nusselt numbers were found only in limited cases compared to smooth fin tubes.

INTRODUCTION

The main focus of the present paper is a particular type of enhancement device: internally finned tubes combined with surface roughness. As indicated by Bergles *et al.* [1], compound enhancement techniques could result in much higher heat transfer increases than when those techniques are applied individually because of synergistic effects of each enhancement technique.

An early experimental investigation on the effects of surface roughness on pressure drop and velocity distribution was performed by Nikuradse [2]. One of the earliest experimental studies on the effect of roughness on heat transfer was done by Cope [3]. A more complete study of surface roughness effects including Prandtl number was done by Dipprey and Sabersky [4]. They developed a similarity rule for heat transfer correlation which is an extension of Nikuradse's approach for friction. Recently, Chyu *et al.* [5] obtained local heat transfer measurements on rough surfaces which had five basic roughness geometries (cylinder, diamond, cube, pyramid and hemisphere), and they provided an in-depth physical explanation on the role played by roughness elements. In general, increases in Nusselt numbers were up to double that of the smooth surfaces and the most favorable situation occurs in the transition region where the friction factor increase could be smaller than the Nusselt number increase.

There is also a considerable amount of literature on the performance of internally finned tubes under laminar and turbulent flow conditions. For example, Shome [6] provide in-depth current

knowledge of single-phase flow in internally finned tubes. An excellent review on existing smooth fin tube correlations can be found in Vlakancic [7]. According to the literature, the maximum increases in both the friction factor and Nusselt number of the finned tubes are expected to be around three times the corresponding values for the smooth tubes.

For the smooth fin tube correlations, the Carnavos correlation [8, 9] has been considered as the state-of-art, based on carefully obtained experimental data for air, water, and water-glycol mixtures with more than twenty internally finned tubes. Recently, Vlakancic [7] investigated fifteen internally finned tubes for both heating and cooling under turbulent flow conditions. Based on his experimental data, Vlakancic [7] found that the Carnavos correlations have some drawbacks. Vlakancic [7], using his own data, proposed improved correlations for internally finned tubes. His own and the Carnavos friction factors were predicted generally within $\pm 12\%$ and Nusselt number data generally within $\pm 15\%$ for both tall fin tubes (which were above the geometrical range of the tubes tested by Vlakancic [7]) and microfin tubes.

The objective of this investigation is to determine how much synergy occurs when finning and roughness are used together. This can be done by comparing the data of rough fin tubes with the performance of matching smooth fin tubes. The Carnavos [8, 9] and Vlakancic [7] smooth fin tube correlations for both friction factor and Nusselt number are used as our reference cases.

EXPERIMENTAL APPARATUS AND PROCEDURE

Flow Loop

The experimental air loop is shown schematically in Figure 1. The flow loop was designed to allow for multiple test section configurations (examining both internal and external flows) using combustion gases (primary flow) and heated air (secondary flow) as the working fluids. This burner/combustion system is capable of maintaining constant temperatures to within $\pm 4^\circ\text{C}$ at the combustion chamber outlet over the entire range of operating flow rates and temperatures. Details can be found in Kim [12].

Test Sections

A total of 13 silicon carbide (SiC) tubes and one smooth metal tube were tested in this project. Parameters of importance are given in Table 1 and an idealized schematic is given on Figure 2. The roughness was caused by the size of the SiC grains and was not controlled. The roughness elements are packed

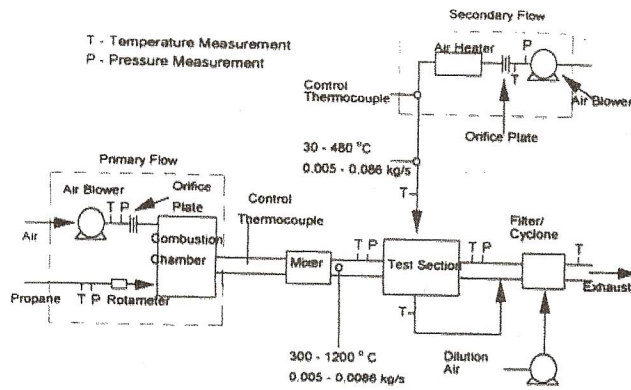


Figure 1. Schematic of the test loop.

very closely, and information concerning microscopic shapes of the roughness elements is not available.

The test tubes' heated/instrumented length was about 1.3m. Located upstream of the test section was a smooth entrance section (0.3m) and flow straighteners were located in it to damp out disturbances.

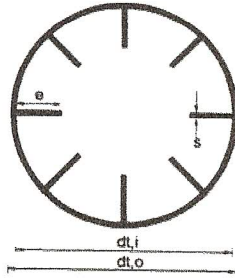


Figure 2. Typical geometry of an internally finned tube.

Instrumentation

Chromel-alumel 30 gage thermocouples were used throughout the apparatus and test sections. Temperature measurements were referenced with a ice point accurate to 0.02°C. Because of the high temperature, large temperature differences in the test sections, and radiation from the combustion gas, radiation shielding of the thermocouples was important to get accurate temperature readings. An Inconel honeycomb (2 mm cells, 25 mm long) was used for the shielding. For the gas bulk temperatures, four or five thermocouples were spaced across the outlet flows on both the tube and shellsides inside the honeycomb. These thermocouples were located just downstream of flowmixers.

Primary and secondary air flow rates were measured using two ASME sharp-edged orifice meters. Pressure drop across the orifice plates was measured using pressure transducers calibrated using a precision alcohol micromanometer. Propane flow rate was measured with precision rotameters.

The energy balance was monitored during the data acquisition, and agreement between the enthalpy loss on the shellside and the enthalpy gain on the tube side was generally within ±5% over the entire range of temperatures and flow rates, except at very low tube side flowrates where the mixer efficiency decreases.

Data Acquisition And Reduction

All the friction factor and heat transfer data were calculated based on the nominal diameter of the tube (or fin root diameter) and bulk fluid temperature (see Marner *et al.* [10]).

The adiabatic friction factor data were taken first using air at room temperature before the heated test section was assembled. After complete assembly of the test section, the shellside inlet temperature was set to 450°C and the flow rate in the shell side was fixed at about 0.059 m³/s.

The tubeside friction factor is calculated as follows:

$$f = \frac{\frac{\partial P}{\partial z} d_{t,i}}{\frac{1}{2} \rho_i \bar{u}_i^2} \cong \frac{\frac{\Delta P}{L_p} d_{t,i}}{\frac{1}{2} \rho_i \bar{u}_i^2} \quad (1)$$

where

$$\bar{u}_i = \frac{4 \dot{V}}{\pi d_{t,i}^2} \quad [\text{m/s}] \quad (2)$$

and L_p is the axial distance between two pressure tap stations.

The tubeside Nusselt numbers were calculated using a Wilson plot technique (see Shah [11]) The overall heat transfer coefficient, U , was defined as:

$$U = \frac{\dot{Q}_{total}}{\Delta T_{ln} A_{t,i}} \quad [\text{W/m}^2/\text{K}] \quad (3)$$

where

$$\dot{Q}_{total} = \frac{\dot{Q}_t - \dot{Q}_s}{\pm} \quad [\text{W}] \quad (4)$$

$$\Delta T_{ln} = \frac{(T_{s,o} - T_{t,i}) - (T_{s,i} - T_{t,o})}{\ln \left(\frac{T_{s,o} - T_{t,i}}{T_{s,i} - T_{t,o}} \right)} \quad [\text{K}] \quad (5)$$

$$A_{t,i} = \pi d_{t,i} L_h \quad [\text{m}^2] \quad (6)$$

where L_h is the heat transfer length.

\dot{Q}_t and \dot{Q}_s are the tubeside and shellside heat transfer rates, respectively

$$\begin{aligned} \dot{Q}_t &= (\dot{m} c_p (T_o - T_i))_t \quad [\text{W}] \\ \dot{Q}_s &= (\dot{m} c_p (T_i - T_o))_s \end{aligned} \quad (7.8)$$

The fin efficiencies of the fin tubes are approximately 100% (as was determined from the high conductivity of the material and relatively low heat transfer coefficient). Hence, the tubeside thermal resistance is given by:

$$R_t = \frac{1}{U A_{t,i}} - R_w = \frac{1}{h_s A_{s,i}} \quad [\text{K/W}] \quad (9)$$

where

$$R_w = \frac{1}{2 \pi \lambda_s L_h} \ln \left(\frac{d_{t,o}}{d_{t,i}} \right) \quad [\text{K/W}] \quad (10)$$

$A_{s,i}$ is the shell side heat transfer area based on the shell inside diameter and h_s is the shellside heat transfer coefficient determined from a correlation based on hydraulic diameter originally given by Dittus-Boelter [15] for turbulent flow in an annular duct as (for shellside cooling):

$$\alpha_s = \frac{\lambda_g}{d_{s,h}} (0.023 (\text{Re}_{s,h})^{0.1} (\text{Pr}_s)^n) \quad [\text{W/m}^2/\text{K}] \quad (11)$$

with $n=0.3$.

Table 1. Geometry of all ceramic tubes and smooth tube tested

TUBE	d_o [10 ⁻³ m]	d_i [10 ⁻³ m]	e [10 ⁻³ m]	s [10 ⁻³ m]	N	H	γ [degree]	Ra_{fi} [10 ⁻³ m]
Smooth	70.03	63.26	-	-	-	-	-	-
IX01	69.13	63.72	-	-	-	-	-	7.95
IX02	68.79	63.44	5.9	3.76	18	0.186	13.5	9.03
IX03	68.8	63.4	5.98	3.49	18	0.189	26	13.2
IX04	68.87	63.4	5.86	3.68	18	0.185	0	7.56
IX05	68.13	62.36	8.4	4.21	18	0.269	0	14.9
IX06	69.03	63.44	5.9	2.28	30	0.186	20	12.2
IX07	68.79	63.86	5.31	1.99	40	0.166	24	11.5
IX08	69.34	63.56	6.04	2.66	30	0.19	0	9.73
IX09	69.07	63.44	6.1	2.59	30	0.192	15.5	14.5
IX10	62.38	52.04	1.22	1.17	60	0.047	0	12.8
IX11	63.23	53.04	1.48	1.28	60	0.056	11.7	8.77
IX12	63.13	54.24	2.04	2.43	30	0.075	0	11.9
IX13	63.17	53.85	2.06	2.33	30	0.077	17	13

From the tubeside thermal resistance, the tube side Nusselt number, based on the inside diameter is:

$$Nu_{exp} = \frac{hd_i}{\lambda_{fi}} \quad (12)$$

Nu_{exp} is experimental Nusselt number and is not corrected for entrance. The correction for variable property effects, $(T_w/T_{b,i})^n$, also was not used since all tests (smooth and finned) were run with approximately the same values of T_w and $T_{b,i}$. Because there is some question as to the value of n for enhanced tubes [6], we thought it prudent to not include this corrector.

Uncertainties of the measured f and Nu_{exp} were typically within $\pm 4\%$ and $\pm 10\%$, respectively.

RESULTS AND DISCUSSION

Smooth Metal Tube Results

The friction factors showed characteristics typical of turbulent flow and they are given in Figure 3. Friction factors ranged from +11% to +1% higher than the reference friction factor correlation. The smooth tube correlation used is that by Filonenko (see Kakac [13]):

$$f = 4[1.58 \ln Re - 3.28]^{-2} \quad (13)$$

As the Reynolds number reached about 44,000, the agreement with equation (13) was within $\pm 2\%$.

The smooth tube Nusselt numbers measured for a heating situation are presented in Figure 4 and show reasonable agreement with the Dittus-Boelter [14] correlation with $n=0.4$. In the Re range of $8,000 < Re < 40,000$, the experimental Nusselt numbers agreed with equation (11) within $\pm 10\%$.

Rough Ceramic Tube Without Fins

One rough ceramic tube without fins (IX01) was tested. Figure 3 shows that the friction factor increases with increasing Re , becoming nearly independent of Re at $Re \geq 60,000$. Nusselt numbers (Figure 4) show that at low Re , the experimental Nusselt numbers compared to the smooth tube Nusselt numbers are relatively larger than those at higher Re , and approach the slope of the smooth Nusselt number curve. This trend is consistent with many data from the literature (see, for example, Cope [3]).

Finned Ceramic Tubes

The twelve internally finned tubes with roughness were tested for $7,500 < Re < 43,000$ for Nusselt numbers, $9,100 < Re < 54,000$ for friction factors, and $Pr \approx 0.7$. Unfortunately, direct comparison of the present data to data from experiments with smooth fin tubes was not possible because smooth fin tubes of identical geometry were not available.

Friction Factor. All the experimental friction factors are presented in Figure 3. Overall, friction factors for these tubes are not only displaced higher (+137% to +1570%) than the friction factors of the smooth metal tube, but also the slopes of the curves are not parallel to that of the smooth metal tube. These trends are not observed with smooth finned tubes (e.g., Vlakancic [7]) with the same H . Physically, these friction factor curves can be considered to occur due to a contribution of the friction factor of a corresponding smooth fin tube plus an additional factor caused by the surface roughness.

The effect of H can be observed between IX05 ($H=0.269$, $N=18$) and IX04 ($H=0.185$, $N=18$); the friction factors of IX05 are much higher than those of IX04. Comparing IX03 ($H=0.189$ and $\gamma=26^\circ$) with IX05, H seems to affect friction factor more strongly than γ does considering that IX05 is a straight finned tube. The effect of γ is relatively straightforward and can be observed from tubes IX02, IX03 and IX04 (very close fin parameters with varying γ): the friction factors increase as γ increases. IX07 showed the highest friction factors (almost 16 times that of the smooth tube friction factor) in this investigation and has the highest e/p and the second highest γ with midrange roughness. Along with IX06 and IX09, this suggests that when there is not enough space between fins (high e/p) such that high velocity fluid cannot reach far into spaces between fins, the presence of γ could pose a significant increase in form drag resulting in high friction factor.

Tubes IX10, IX11, IX12 and IX13 have considerably smaller H (< 0.077) than the other tubes. The friction factors were considerably lower than those of the rough finned tubes with higher H . The friction factors were less than 5 times the smooth metal tube friction factors, and the data trends are closer to the

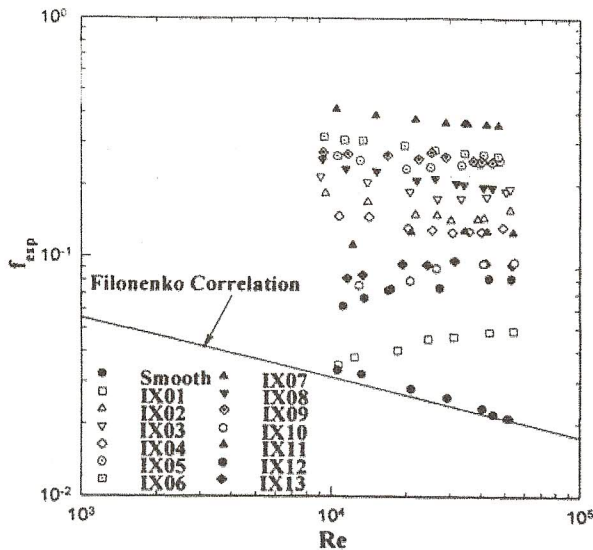


Figure 3. Overall friction factor data

characteristics of tube IX01 (rough tube without fins) rather than the typical rough fin tubes with higher H . The friction factors increase until a certain Re is reached and then become almost independent of Re . This fact might indicate that the physics of the flow in this group of tubes would be governed mostly by the roughness, and the role of the fins would be weak.

Nusselt Numbers. The Nusselt number results for these tubes are displayed in Figure 4. Relatively large increases in Nusselt number seem to be possible with straight finned tubes (IX04 and IX05) at low Re ; strong effects of thermally developing flow (increasing slope of Nusselt number curve with respect to increasing Re ; much higher Nusselt numbers at lower Re and asymptotic approach to the slope of the smooth tube Nusselt numbers as Re increases) were observed with IX04 and IX05. Considering the variation of the Nusselt number slope, the developing length in a straight fin tube is expected to be generally longer than that of a helical fin tube especially at low Re (thermal entry length for smooth pipe is known to be approximately 10–15 times the diameter but it was not measured for the fin tubes tested in this investigation).

Comparing a group of tubes IX02, IX03, IX04 and IX05 which have $N=18$, IX05 shows the smallest increase in Nusselt numbers (around 30% at $Re=35,000$) although it shows the largest friction factor increase (over +650%) in this group of tubes considered. This might suggest that the fin area has not been used effectively for heat transfer because of the highest roughness ($14.94 \mu m$) combined with the highest $H=0.269$. The depth to which higher velocity flow would reach between two adjacent fins would be deeper for IX04 than that of IX05 resulting in more effective heat transfer area although IX05 has more actual heat transfer area. Similar physical explanations are possible for IX02 and IX03 in their overall heat transfer performance.

It is noteworthy that Nusselt numbers for IX07 are not the highest while its friction factors are the highest. These inconsistencies between the order of friction factor increase and Nusselt number increase are also found between IX06 and IX08. This phenomenon implies that when the fluid flows over fin surface, there is large loss of momentum (via form drag) and as a consequence, the flow velocity becomes considerably lower

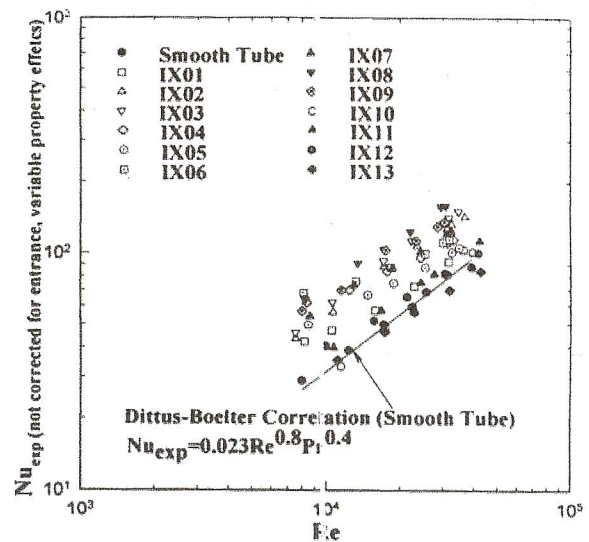


Figure 4. Overall Nusselt number data

without promoting desired turbulence such as swirling and separation. These effects would increase as γ , H , Re and roughness increase which are mainly responsible for the form drag increase especially with $N=30$ or more, and results in low effective heat transfer area. Consistent with the above explanations, IX08 ($\gamma=0^\circ$) turns out to be the best performer in terms of Nusselt number increase (+115%) with relatively smaller increase in friction factor.

Tubes IX10, IX11, IX12 and IX13 have $N=30$ or 60 and $H \leq 0.076$. They show the overall lowest Nusselt number enhancement among the tubes compared to the previous ones. The Nusselt number increase ranged from -15% to 20% over the smooth tube Nusselt numbers. Some of these experimental results were rather surprising because the Nusselt numbers for tubes IX10 and IX13 were lower than a smooth metal tube. The tubes in this group have about the same roughness as the rest of the tubes considered in this study (IX02 through IX09).

Considering that the nominal inside diameters of the tubes in this group are about 20% less than those of the rest of the tubes, the same roughness means the size of the roughness element is relatively larger compared to the fin size. Therefore, the effects of the roughness is much stronger than those in tall fin tubes and the effective heat transfer area might be decreased significantly, probably equivalent to a smooth tube (with no fin) of smaller diameter. This suggests that the rough microfin tube loses its advantage compared to a smooth microfin tube, and results in overall poor performance.

Among many aspects of heat transfer enhancement mechanisms with finned tubes, the trade-off between the increased heat transfer area and the flow resistance caused by the fins is believed to dictate the overall heat transfer performance. For heat transfer enhancement, the utilization of the increased surface area due to adding fins primarily depends on the amount of the flow passing through the area between fins. Also, separations, induced by helical fins, might be a contributory factor, although it is hard to quantify the amount of contribution to the total performance.

Microfin tubes have many small fins (typically $H < 0.06$ and more than $N=30$ according to Vlakancic [7]) and from the view point of the flow, microfins pose relatively negligible inter-fin flow resistance because the fin height is very small. Therefore, it is

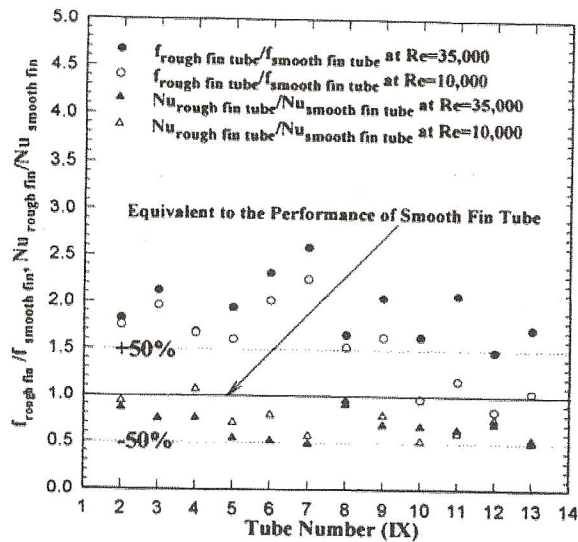


Figure 5. Performance comparison of rough fin tubes using the Carnavos smooth fin tube correlations

very likely that the flow fully uses the increased surface area between the fin, although the pitch of micro fin tubes is typically much smaller than that of tall fin tubes due to the increased N .

As an alternative to the above given physical explanation, it would be more convenient to introduce an idea of "penetration depth" than mentioning the above given physical reasons repeatedly.

The penetration depth is the depth to which "higher" velocity flow reaches between two adjacent fins (The penetration depth concept is used only qualitatively in this paper and is under numerical investigation). The fin area below this "penetration depth" is not fully effective for heat transfer. Thus, the effective area for heat transfer is less than the actual heat transfer area. The heat transfer contribution of this low velocity area is probably very small compared to the contribution made by the area where the velocities are greater.

Comparisons With Smooth Fin Tube Correlations

Performance comparisons of rough fin tubes to smooth fin tubes (with the same geometry except the roughness) are presented in Figures 5 and 6. The range of Re used in these figures is $10,000 < Re < 35,000$. For Nusselt numbers for IX10, the Carnavos correlation was used because Vlakancic's correlation does not predict microfin tubes with straight fins.

Friction Factor. Good agreement between the two smooth fin correlations can be found in some tubes (IX02 and IX03) but the Vlakancic correlation generally indicates more increase in rough fin tube friction factors over smooth fin tube than the Carnavos correlation. Note that the friction factors of IX10 and IX12 are lower than those of smooth fin tubes and, they do not make physical sense because the friction factors of the rough fin tubes should be higher than smooth tube friction factors due to the contribution by the roughness. Thus, this calls into question the Carnavos correlation for these tube geometries. Therefore, Vlakancic's predictions are believed to be more accurate, and the increases due to the roughness ranged from +100 to +280% over smooth fin tube friction factors at higher Re .

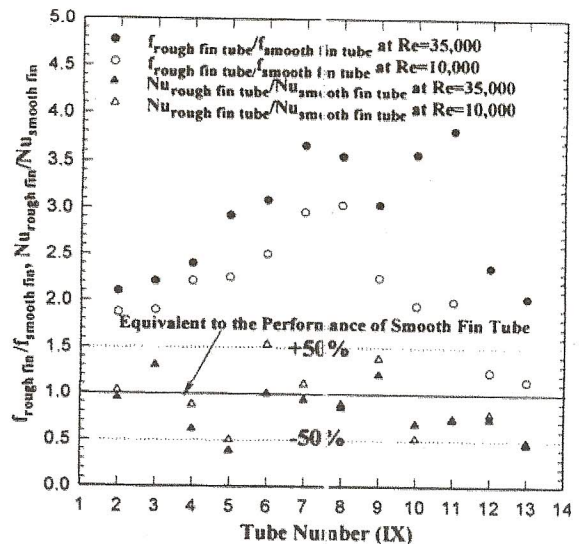


Figure 6. Performance comparison of rough fin tubes using the Vlakancic smooth fin tube correlations

Nusselt Number. In general, Figures 5 and 6 show better agreement for the Nusselt numbers (generally in $\pm 50\%$ band) than for the friction factors. The commonality in both Figures 5 and 6 is that there are synergistic effects caused by roughness depending on proper selection of fin geometry, but in general, Nusselt number increases caused by the roughness are often accompanied by even larger increases in friction factors. The maximum increase in Nusselt number is +50% over smooth fin tube Nusselt number and is found with IX06 at lower Re . Synergistic effects at higher Re can be found in IX03 and IX09 also, but the corresponding increases in Nusselt Numbers are less than +30%. IX06 and IX09 show that they would be much better at low Re and the enhancement could be +50% or more.

SUMMARY AND CONCLUSIONS

Overall, the increase in friction factor for rough fin tubes was from +137% to +1570% compared to smooth metal tubes, and the increase ranged from +100% to +280% when compared to those of geometrically equivalent smooth fin tubes at higher Re . The increase in Nusselt numbers for rough fin tubes was -15% to +115% compared to smooth metal tubes, and the increase ranged was around -50% to +50% when compared to those of equivalent smooth fin tubes over the range of Re , $10,000 < Re < 35,000$.

A summary of the observations on the friction factors and Nusselt numbers of rough fin tubes can be made:

1. Physically, the friction factors can be thought as the superposition of a developing friction factor of a corresponding smooth fin tube plus a friction factor caused by the surface roughness.
2. The most dominant parameter in the friction factor increase is e/p when H is large (within the measured roughness range of this study).
3. Straight fin tubes have a large potential for increases in Nusselt numbers, especially at lower Re when the fin height is relatively large (IX04 and IX05).
4. For micro fin tubes (IX10, IX11, IX12 and IX13), both friction and heat transfer are governed primarily by the roughness rather than γ .
5. Smaller roughness with moderate fin height ($H \geq 0.08$) leads to increase Nusselt numbers.

6. For H greater than 0.166, the use of helix angle is not recommended unless $Re < 10,000$.

ACKNOWLEDGMENTS

Financial support from the New York State Energy Research and Development Authority is gratefully acknowledged. The authors are grateful to INEX Inc. for supplying the ceramic tubes.

NOMENCLATURE

A	(nominal) flow area of an internally finned tube; surface area [m ²]
c_p	specific heat at constant pressure [J/kg·K]
d_i	inner, nominal diameter of tube [m]
e	fin height [m]
f	friction factor based on nominal inside diameter
α	heat transfer coefficient, based on nominal heat transfer area [W/m ² -K]
H	non-dimensional fin height [=2e/di]
λ	thermal conductivity [W/m-K]
L_p	tube length between pressure taps [m]
L_h	heat transfer length [m]
\dot{M}	mass flow rate [kg/s]
N	number of fins
Nu_{exp}	experimental Nusselt number based on nominal tube diameter [$\alpha d_i / \lambda$], not corrected for entrance effects
p	fin pitch [m]
Pr	Prandtl number [$c_p \eta / k$]
\dot{Q}	heat duty [W]
\dot{V}	volumetric flow rate [m ³ /s]
s	mean fin thickness [m]
\bar{u}	mean axial velocity based on tube nominal diameter [m/s]
R	thermal resistance [K/W]
Ra	surface roughness, arithmetic mean of departures of a measured profile of rough surface from the mean line [μm]
Re	Reynolds number based on nominal tube diameter [$\rho \bar{u} d_i / \eta$]
T	temperature [K]
U	overall heat transfer coefficient [W/m ² -K]

Greek Symbols

ΔT_{ln}	log-mean temperature difference [K]
γ	fin helix angle [degrees]
η	dynamic viscosity [Pa-s]
ρ	fluid density [kg/m ³]

Subscripts

i	inner, inlet in T
o	outer, outlet in T
$ _t$	tube side
$ _s$	shellside
w	wall

REFERENCES

- Bergles, A. E., Jensen, M. K., and Shome, B., 1995, Bibliography on Enhancement of Convective Heat and Mass Transfer," HTL-23, Rensselaer Polytechnic Institute, Troy, NY.
- Nikuradse, J., 1933, Laws for Flow in Rough Pipes, *VDI-Forschungsch*, no. 361, Also available as NACA Tech Memo 1292.
- Cope, W. F., 1941, The Friction and Heat Transmission Coefficients of Rough Pipes, *Proc. Institution of Mechanical Engineers*, Vol.145, pp.99-105.
- Dipprey, D. F. and Sabersky, R. H., 1963, Heat and Momentum Transfer in Smooth and Rough Tubes at Various Prandtl Numbers, *Int. Journal of Heat and Mass Transfer*, Vol. 6, pp. 329-353.
- Chyu, M. K. and Natarajan, V., 1996, Heat Transfer on the Base Surface of Three Dimensional Protruding Elements, *Int. J. Heat and Mass Transfer*, Vol. 39, pp. 2925-2935.
- Shome, B., 1995, Experimental and Numerical Investigation of Variable Property / Mixed Convection Laminar Flow in Internally-Finned Tubes, Ph. D. Thesis, Rensselaer Polytechnic Institute, Troy, NY.
- Vlakancic, Alex, 1996, Experimental Investigation of Internally-Finned Tube Geometries on Turbulent Heat-Transfer and Fluid Flow, M.S. Thesis, Rensselaer Polytechnic Institute, Troy, NY.
- Carnavos, T. C., 1979, Cooling Air in Turbulent Flow with Internally Finned Tubes, *Heat Transfer Engineering*, Vol. 1., No. 2, pp. 41-46.
- Carnavos, T. C., 1980, Heat Transfer Performance on Internally Finned Tubes in Turbulent Flow, *Heat Transfer Engineering*, Vol. 1., No. 4, pp. 32-37.
- Marnier, W. J., Bergles, A.E., and Chenoweth, J. M., 1983, On the Presentation of Performance Data for Enhanced Tubes Used in Shell-and-Tube Heat Exchangers, *J. Heat Transfer*, Vol. 105, pp. 358-365.
- Shah, R.K., 1990, Assessment of Modified Wilson Plot Techniques for Obtaining Heat Exchanger Design Data, *Heat Transfer, Proc. of 9th Int. Heat Transfer Conf.*, Hemisphere Publishing, NY, Vol. 5, pp. 51-56.
- Kim, Je-Hoon, 1996, Experimental Investigations of Internally Finned Tubes with Roughness on Turbulent Heat Transfer and Fluid Flow, M.S. Thesis, Rensselaer Polytechnic Institute, Troy, NY.
- Kakac, S., 1987, The effect of Temperature Dependent Fluid Properties on Convective Heat Transfer in, *Hand Book of Single-Phase Convective Heat Transfer*, John Wiley, NY.
- Dittus, P. W., and Boelter L. M. K., 1930, Heat Transfer in Automobile Radiators of the Tubular Type, *Int. Communications in Heat and Mass Transfer*, Vol. 12, pp. 3-22.